Supporting Information

Boosting NIR-Driven Photocatalytic Activity of BiOBr:Yb^{3+}/Er^{3+}/Ho^{3+} Nanosheets by Enhanced Green Upconversion Emissions via Energy Transfer from Er^{3+} to Ho^{3+} Ions

Yongjin Li,[†] Zhiyuan Cheng,[†] Lu Yao,[†] Shenghong Yang,[‡] and Yueli Zhang[*,†]

[†]State Key Laboratory of Optoelectronic Materials and Technologies, School of Materials Science and Engineering, Sun Yat-Sen University, No. 135, Xinggangxi Road, Guangzhou 510275, China

[‡]School of Physics, Sun Yat-Sen University, No. 135, Xinggangxi Road, Guangzhou 510275, China

[*]Corresponding Author: stszyl@mail.sysu.edu.cn.

Number of pages: 11

Number of Tables: 1

Number of Figures: 11

Characterization

X-ray diffraction (XRD) was characterized by Rigaku Smartlab diffractometer. Transmission electron microscopy (TEM) images were obtained using a FEI Tecnai G2 F30 and G2 Spirit. X-ray photoelectron spectroscopy (XPS) tests were performed in an ESCALAB 250 spectrometer. Electron paramagnetic resonance (EPR) spectra were recorded by Bruker A300. Fourier transform infrared absorption (FT-IR) was detected by NICOLET 6700. The N_2 adsorption/desorption measurements were by ASAP 2020. The UV–Vis–NIR absorption spectra were obtained by UV3600 spectrophotometer. The photoluminescence and lifetimes were performed in Edinburgh FLS980 spectrometer. Photocurrent analysis and electrochemical impedance spectroscopy were conducted using CHI760E electrochemical workstation.

Calculations

In the present work, the calculations are performed using the CASTEP module within the plane-wave pseudopotential method, along with the generalized gradient approximation (GGA) exchange and correlation function in the scheme of Perdew-Burke-Ernzerhof (PBE).[1-3] The convergence tests regarding the cutoff energy have been made before the calculations of the properties and a plane wave cutoff energy of 480eV is used. Ultrasoft pseudopotential is adopted in the reciprocal space, and 2×2×2 Monkhorst–Pack mesh grid is sufficient to reach convergence for 2×2×1 supercell calculations. All the atoms of the pure BiOBr and oxygen vacancies with BiOBr are fully relaxed to their equilibrium positions with an energy convergence of

5×10^{-6} eV while the force applied on each atom is less than 0.01 eV/Å and the stress is less than 0.02 GPa. In addition, the atomic displacement is less than 5×10^{-4} Å and the self-consistent field (SCF) tolerance is 2×10^{-6} eV.

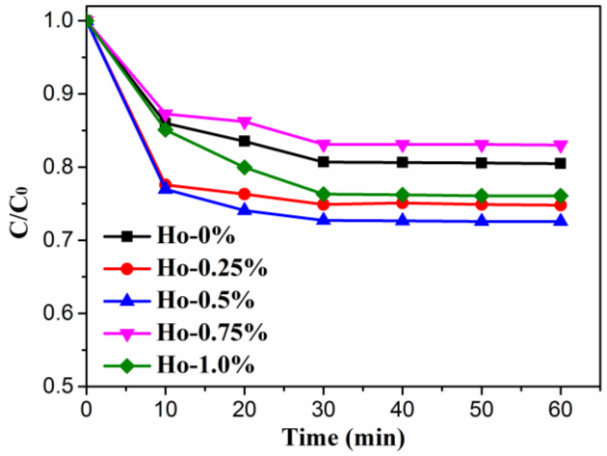

Figure S1. Adsorption property of BiOBr:Yb^{3+}/Er^{3+}/Ho^{3+} nanosheets with different Ho^{3+} concentrations.

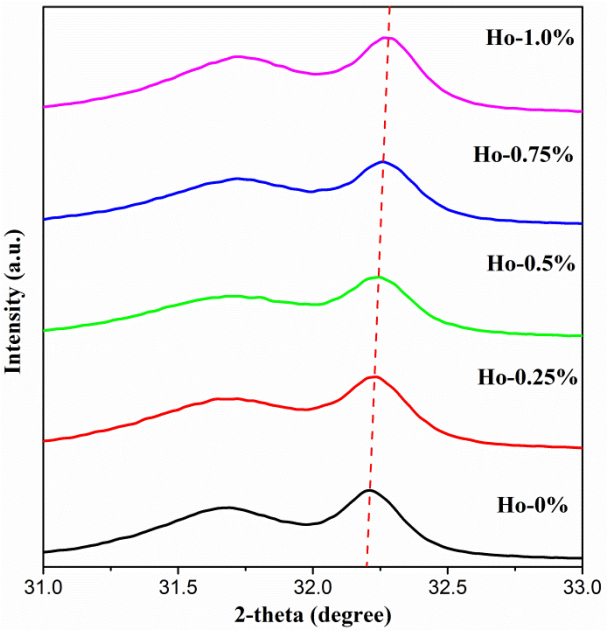

Figure S2. The main diffraction peak near 2θ =31° - 33° of the BiOBr:Yb^{3+}/Er^{3+}/Ho^{3+} nanosheets with different Ho^{3+} concentrations.

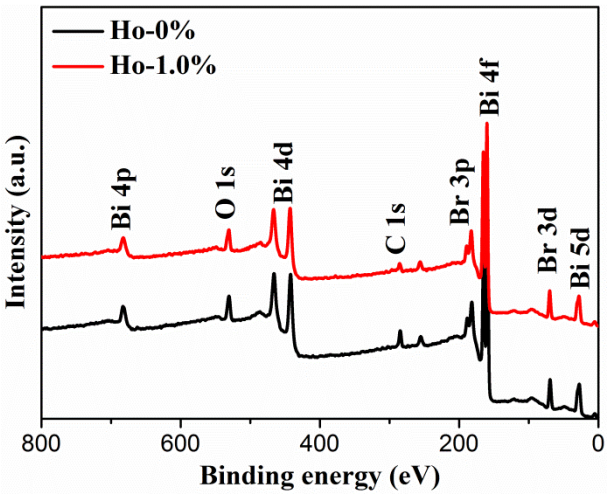

Figure S3. XPS survey spectra of BYE-0Ho and BYE-1.0Ho.

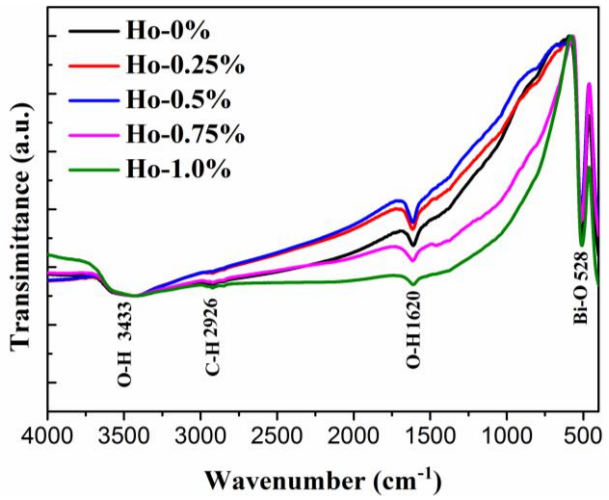

Figure S4. FT-IR spectra of BiOBr:Yb^{3+}/Er^{3+}/Ho^{3+} nanosheets with different Ho^{3+} concentrations.

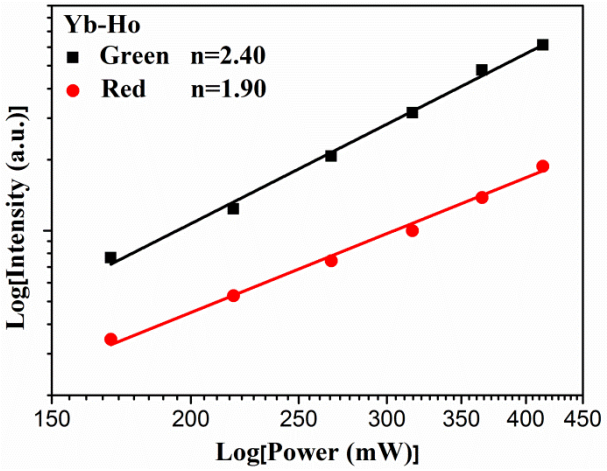

Figure S5. The double logarithmic curve of green and red luminescence intensity dependence on pump power of BiOBr: Yb^{3+}/Ho^{3+}.

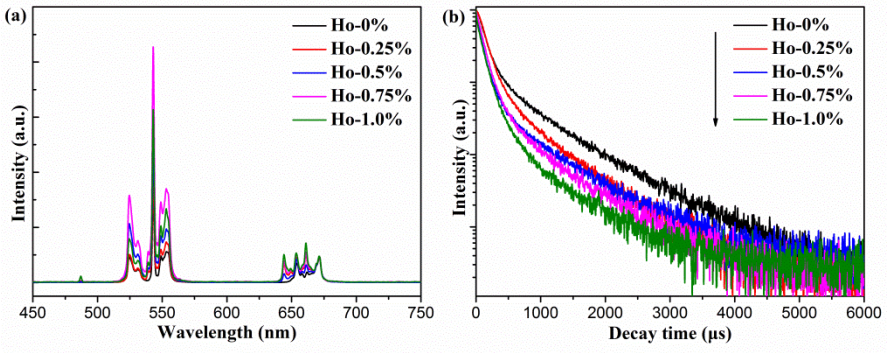

Figure S6. UC luminescence spectra and (b) The decay curves of $^4F_{9/2}$ level (Er^{3+}) of BiOBr: Er^{3+}/Ho^{3+} nanosheets with different Ho^{3+} contents excited by 980 nm.

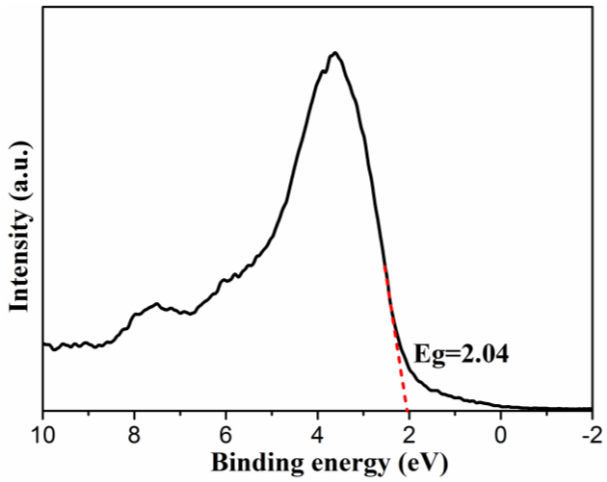

Figure S7. VB-XPS spectra of BYE-0.5Ho.

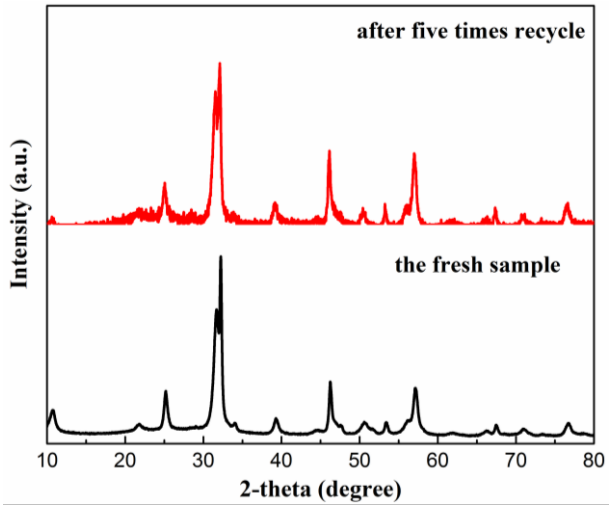

Figure S8. XRD pattern of BYE-0.5Ho before and after photocatalytic reaction.

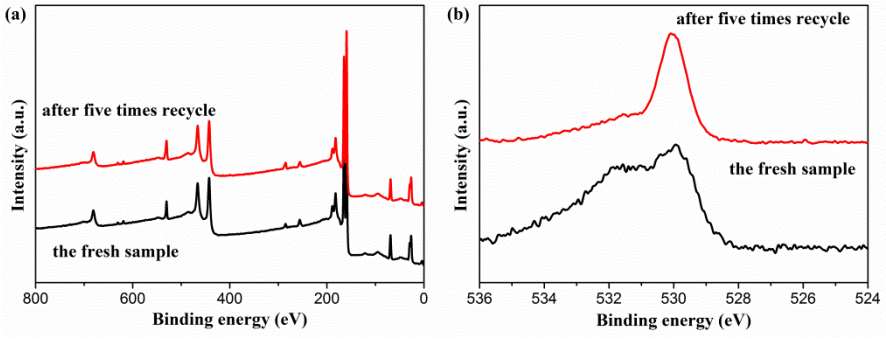

Figure S9. XPS spectrum of BYE-0.5Ho before and after photocatalytic reaction (a) survey and (b) O.

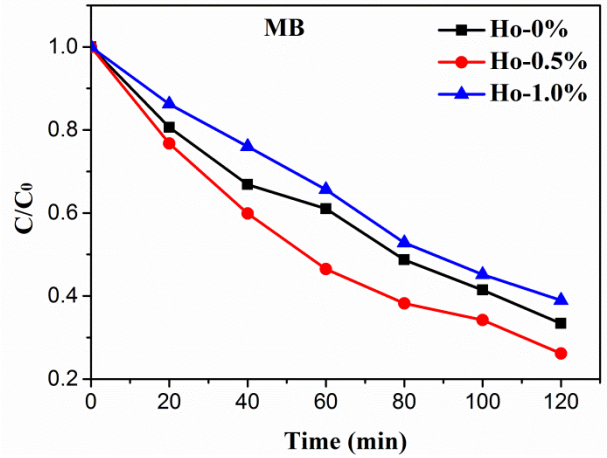

Figure S10. Photodegradation of MB of all samples under UV-Vis-NIR light irradiation.

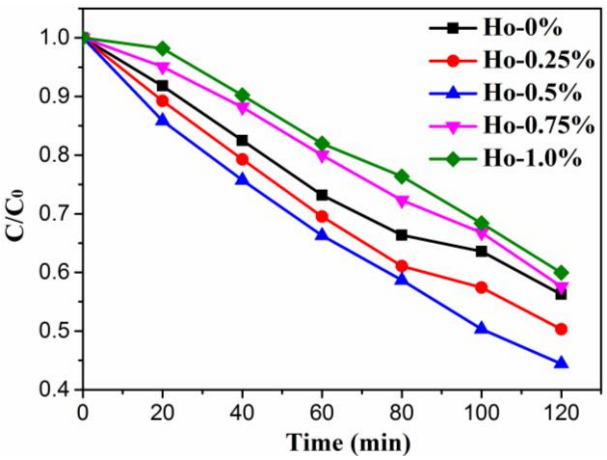

Figure S11. Photodegradation of BPA of all samples under UV-Vis-NIR light irradiation.

Table S1. Structural details of BiOBr:Yb^{3+}/Er^{3+}/Ho^{3+} nanosheets with different Ho^{3+} concentrations by Rietveld refinement.

Sample	BYE-0Ho	BYE-0.5Ho	BYE-1.0Ho
Crystal system	Tetragonal	Tetragonal	Tetragonal
Space group	P4/nmm (no. 129)	P4/nmm (no. 129)	P4/nmm (no. 129)
Lattice parameters			
a =b (Å)	3.9303(19)	3.9266(5)	3.9254(2)
c (Å)	8.1414(39)	8.1282(14)	8.1266(44)
V ($Å^3$)	125.768(18)	125.326(49)	125.221(16)
Atomic positions			
Bi/Er/Yb/Ho (2c)			
x	0.2500	0.2500	0.2500
y	0.2500	0.2500	0.2500
z	0.1553(3)	0.1538(4)	0.1566(2)
O (2a)			
x	0.2500	0.2500	0.2500
y	0.7500	0.7500	0.7500
z	0.0000	0.0000	0.0000
Br (2c)			
x	0.2500	0.2500	0.2500
y	0.2500	0.2500	0.2500
z	0.6516(8)	0.6574(9)	0.6464(5)
$R_{factors}$ (%)			
R_{Wp}	8.31	9.67	8.83
R_p	6.42	7.72	7.08
χ^2	2.61	3.38	2.98

Reference

1. Perdew, J. P.; Ruzsinszky, A.; Csonka, G. I.; Vydrov, O. A.; Scuseria, G. E.; Constantin, L. A.; Zhou, X.; Burke, K., Restoring the density-gradient expansion for exchange in solids and surfaces. *Phys. Rev. Lett.* **2008**, 100, 136406.

2. Zhao, Z.; Liu, Q.; Dai, W., Structural, Electronic, and Optical Properties of $BiOX_{1-x}Y_x$ (X, Y= F, Cl, Br, and I) Solid Solutions from DFT Calculations. *Sci. Rep.* **2016**, 6, 31449.

3. Wang, Q.; Liu, Z.; Liu, D.; Liu, G.; Yang, M.; Cui, F.; Wang, W., Ultrathin two-dimensional $BiOBr_xI_{1-x}$ solid solution with rich oxygen vacancies for enhanced visible-light-driven photoactivity in environmental remediation. *Appl. Catal. B: Environ.* **2018**, 236, 222-232.